

Transformable Gaussian Reward Function for Socially-Aware Navigation with Deep Reinforcement Learning

Jinyeob Kim¹, Sumin Kang², Sungwoo Yang², Beomjoon Kim¹,
Yura Jargalbaatar^{2*}, Donghan Kim^{2*}

¹Department of Artificial Intelligence, College of Software, Kyung Hee
University, Yongin, Republic of Korea.

²Department of Electronic Engineering (AgeTech-Service Convergence
Major), College of Electronics & Information, Kyung Hee University,
Yongin, Republic of Korea.

*Corresponding author(s). E-mail(s): jargalbaatar@khu.ac.kr;
donghani@khu.ac.kr;

Contributing authors: wls2074@khu.ac.kr; suminsk@khu.ac.kr;
p1112007@khu.ac.kr; 1222kbj@khu.ac.kr;

Abstract

Robot navigation has transitioned from prioritizing obstacle avoidance to adopting socially aware navigation strategies that accommodate human presence. As a result, the recognition of socially aware navigation within dynamic human-centric environments has gained prominence in the field of robotics. Although reinforcement learning technique has fostered the advancement of socially aware navigation, defining appropriate reward functions, especially in congested environments, has posed a significant challenge. These rewards, crucial in guiding robot actions, demand intricate human-crafted design due to their complex nature and inability to be automatically set. The multitude of manually designed rewards poses issues with hyperparameter redundancy, imbalance, and inadequate representation of unique object characteristics. To address these challenges, we introduce a transformable gaussian reward function (TGRF). The TGRF significantly reduces the burden of hyperparameter tuning, displays adaptability across various reward functions, and demonstrates accelerated learning rates, particularly excelling in crowded environments utilizing deep reinforcement learning (DRL). We introduce and validate TGRF through sections highlighting its conceptual background, characteristics, experiments, and real-world application,

paving the way for a more effective and adaptable approach in robotics. The complete source code is available on <https://github.com/JinnnK/TGRF>

Keywords: Artificial intelligence, Machine learning, Reinforcement learning, Robotic programming, Robots, Reward shaping

1 Introduction

Over the years, the robotics field has shown a persistent interest in robot navigation. Initially, research efforts focused on basic obstacle avoidance and random navigation strategies [1-3]. Advances in navigation techniques led to simultaneous localization and mapping (SLAM) [4-6], where robots estimate their positions and create maps to move effectively. Strategies expanded to address dynamic environments [7-17], as robotics consistently pursued advancements in navigation.

However, despite the integration of robots into human environments, effectively avoiding collisions with humans remains a significant challenge. While safety, performance, and navigation in static environments were previously emphasized [18], the field has now shifted its focus to socially aware navigation, recognized as crucial [12-14, 16, 17]. Socially aware navigation integrates perception, intelligence, and behavior to adhere to social norms [19, 20], necessitating the critical ability to differentiate between humans and static objects.

To deal with this challenge, two main research directions emerged: reactive navigation [9-11, 15] and navigation utilizing reinforcement learning (RL) [21-24]. Reactive navigation responds to real time sensor data, with limitations in foreseeing future movements. RL uses markov decision process (MDP) and deep reinforcement learning (DRL) [12-14, 16, 17, 25], utilizing deep neural networks for well-informed decisions and enabling robots to navigate safely in human environments.

However, the challenges in defining these reward functions become particularly evident in crowded environments where robots navigate [21, 26-28]. These reward functions essentially serve as the guiding principle steering the actions of agents by evaluating the potential value of each action. As a result, human-crafted rewards become indispensable as they can't be automatically set. However, as demonstrated in Fig. 1, inadequately designed reward functions can induce risky behaviors in human-robot interactions. Moreover, the manual design of numerous such rewards presents several critical issues.

First, the proliferation of distinct reward functions for various components in crowded environments necessitates a redundant number of hyperparameters [12-14, 16, 17, 25, 29-31]. Each reward demands tailored functions that align with its specific attributes, be it the distance from humans, the direction towards the goal, or even human intentions. This surplus of reward functions results in excessive fine-tuning of hyperparameters, leading to imbalances in the rewards. These imbalances can inadvertently steer robots towards humans, increasing the risk of collisions [12]. Such disparities in action priorities, caused by reward imbalances pose a significant challenge in tuning hyperparameters and identifying inadequate rewards.

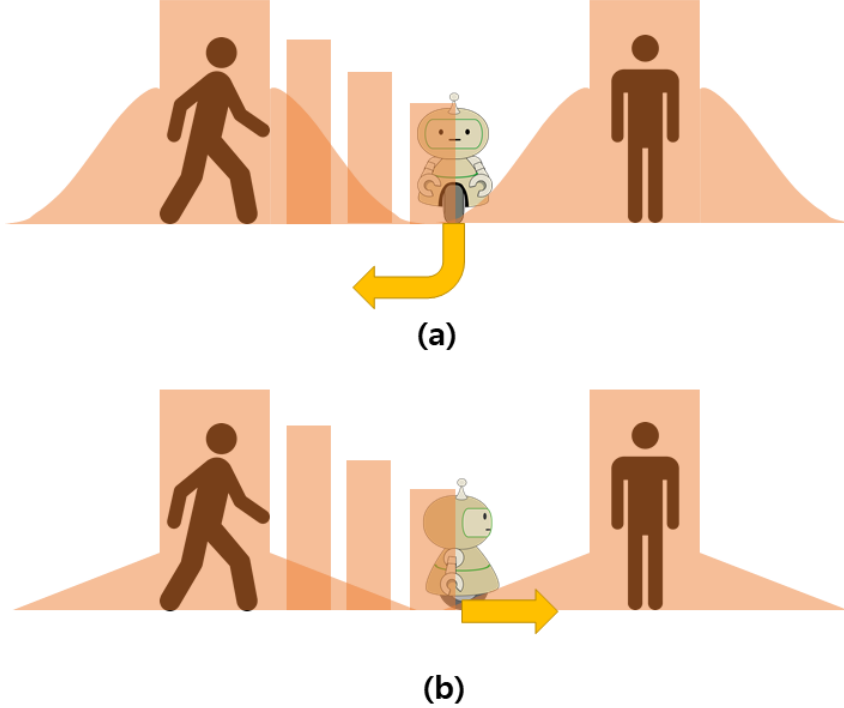


Fig. 1 The robot’s actions when the adequate reward functions are used or not. The red shapes represent penalties, and the yellow arrows indicate the robot’s actions. Penalties are imposed when the robot is in proximity to humans, within their surroundings, or moving in their direction.

Second, the fixed form of each reward function is not temporally and experimentally inefficient. The utilization of static context specific reward functions has been observed [12, 14, 16, 17, 32-35]. However, these often fall short in adequately representing its unique characteristics. Even when the same formula is employed, the diverse attributes may not be accurately captured. This discrepancy demands extensive empirical design and experimentation with specific reward functions to achieve higher performance.

Third, the hurdle can extend to effective learning [27]. Crafting appropriate reward functions with the correct number of hyperparameters remains a significant challenge, leading to collisions and hindering robot learning.

This study proposes a transformable gaussian reward function (TGRF), aiming to guide robots along safer routes. This approach brings several crucial contributions. (1) The less number of hyperparameters significantly alleviates the burden of parameter tuning, expediting the search for an optimal reward function. (2) TGRF demonstrates adaptability to various reward functions through dynamic shape adjustments. Such adaptability stands in stark contrast to previous models [13], which often required extensive redesigns for shape changes. (3) TGRF shows accelerated learning rates, excelling notably in crowded environments, effectively harnessing the potential of DRL.

To demonstrate the performance of TGRF, we introduce key points in reward shaping and relevant papers for comparison in experiments in Section II. In Section

III, we present background knowledge, characteristics of TGRF, and introduces the reward functions using TGRF. In Section IV, we showcase two experiments conducted to demonstrate the performance of TGRF, and present the results of this study’s application in real environments in Section V. Finally, we concludes the paper in Section VI.

2 Related Works

2.1 Integration of Prior Knowledge through Human Delivered Reward Functions

Reinforcement learning is a machine learning approach operating within MDP [21], where an agent interacts with a specific environment, receiving feedback in the form of rewards. The primary objective is to achieve the maximum cumulative reward, driving the learning of policies. The reward function significantly influences the agent’s decision making process, steering it towards converging to optimal policies.

However, a prevalent issue arises as agents typically lack complete information about all aspects of the environment [36]. In vast state spaces, transitions between states and rewards might be unknown or stochastic. Moreover, the agent remains unaware of the consequences and outcomes of actions until they are executed.

As a result, in such scenarios, agents require substantial experience to converge to optimal policies for complex tasks in the absence of prior knowledge. To address this challenge, research in reinforcement learning explores reward shaping, aiming to guide agents towards making better decisions at appropriate times through suitable reward values [27, 28]. This approach aims to significantly reduce the learning time by fostering the convergence to optimal policies without explicit prior knowledge.

Previous studies have extensively explored incorporating prior knowledge into reward functions [26, 28, 37-40]. However, crafting reward functions encompassing general prior knowledge, such as apprehension concerning collision risks based on proximity to humans or progress relative to the destination, is challenging due to various environmental and psychological factors. These factors make it impossible to express such knowledge simply through mathematical formulations.

To address this challenge, recent research has focused on utilizing inverse reinforcement learning (IRL), where humans intervene at intermediate stages to provide rewards [41]. In addition, a study utilizing natural language to communicate intermediate reward functions to agents have emerged [42]. These studies involve humans evaluating the actions of robots as rewards and assigning them accordingly. As a result, they have demonstrated the transmission of rewards imbued with prior knowledge to agents during learning, thereby accelerating the learning process and enhancing algorithm performance.

However, due to their reliance on human intervention, these approaches are unsuitable for environments requiring extensive learning or complex tasks without direct human involvement. Therefore, there is a growing need for research on reward shaping that can consider prior knowledge and deliver high performance without direct human intervention, especially in environments demanding substantial learning.

2.2 Reward Function Analysis for Human Avoidance in Robot Navigation

Recent research has been actively exploring methods for robot navigation in environments where humans and robots coexist [12-14, 16, 17, 25, 29-31]. Their reward functions commonly employ different formulas based on objectives, all without direct human intervention, and can broadly be classified into four types. These include rewards categorized as follows: reaching the destination, $r_{goal}(s_t)$; collision avoidance with humans, $r_{col}(s_t)$; distance from humans, $r_{disc}(s_t)$; and distance from the destination, $r_{pot}(s_t)$.

$r_{goal}(s_t)$ and $r_{col}(s_t)$ usually assume consistent values, while $r_{disc}(s_t)$ and $r_{pot}(s_t)$ encompass numerous formulas reflecting prior knowledge, such as linear, L2 norm, or exponential functions. For instance, $r_{disc}(s_t)$ consistently imposes a larger penalty as the distance between humans and robots diminishes. This design aligns with the psychological theory of Proxemics [20], which evaluates discomfort based on interpersonal distances, integrating prior knowledge about the potential discomfort associated with varying distances between humans and robots.

In addition, $r_{pot}(s_t)$ incentivizes the robot's faster arrival at the destination by applying rewards or penalties based on changes in the L2 norm distance between the robot and the destination. These approaches reflect rational strategies by integrating prior knowledge concerning discomfort levels associated with distances (Proxemics) and apprehensions regarding collision probabilities based on proximity to humans. Moreover, they encourage robots to expedite their arrival at the destination through rewards/penalties based on the changing distance from the destination using the L2 norm.

However, papers related to reward shaping and reinforcement learning argue that it is crucial to verify if the rewards take appropriate forms and maintain suitable proportions [27, 28]. If the shapes of rewards are inadequate for the objectives or overly biased, the robot may steer its learning process in a direction not intended by the algorithm, potentially leading to the freezing robot problem [42]. In addition, an excessive number of hyperparameters might hinder the quest for optimal performance.

The aforementioned prior studies experimentally determined reward functions and the count of hyperparameters. As a result, some were excessively simplistic, preventing researchers from intuitively adjusting rewards through hyperparameters, while others exhibited complex structures that hindered straightforward modifications of hyperparameters. This resulted in significant time consumption to achieve optimal performance and limitations in adjusting inadequate rewards, necessitating redesigns of the reward function.

For instance, in [13], researchers designed simple reward functions with redundant hyperparameters. This led to a substantial nine fold gap between $r_{pred}(s_t)$ and $r_{disc}(s_t)$. This results in situations in which the robot favors actions with smaller penalties from $r_{disc}(s_t)$ over larger penalties from $r_{pred}(s_t)$, thereby resulting in intrusions and collisions.

This directly impacts the learning process, rendering the task of identifying the appropriate reward function and hyperparameters more challenging and requiring formula modifications.

Therefore, this study proposes TGRF, allowing for intuitive and versatile applications with less hyperparameters. By enabling researchers to intuitively adjust rewards, it reduces the time required for exploring suitable reward functions and ensures optimal performance by finely tuning reward balances. To substantiate this claim, we directly compare the reward function utilized in socially aware navigation (SCAN) [16], decentralized structural-RNN (DS-RNN) [17], gumbel social transformer + human-human attention (GST+HH Attn) [13, 43], and crowd aware memory based reinforcement learning (CAM-RL) [31].

3 Suggested Reward Function

In section III-A, we briefly introduce background knowledge regarding the model. Subsequently, in section III-B, we elaborate on the proposed TGRF in this paper. Lastly, in III-B-3, we describe the application of TGRF to the reward functions within the environment and model of [13].

3.1 Preliminaries

3.1.1 Markov decision process (MDP) and navigation methods

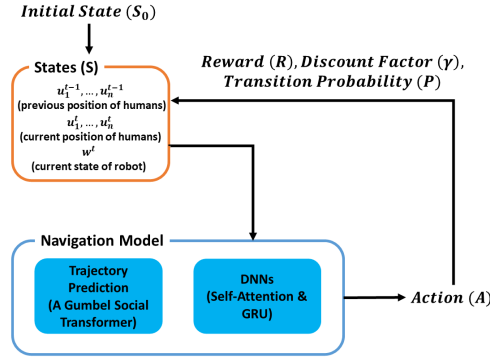


Fig. 2 Diagram of an MDP with the Navigation model applied.

In the crowded environment described by the tuple $\langle S, A, P, R, \gamma, S_0 \rangle$, robots and humans follow distinct policies during simultaneous movements. It includes states (S), actions (A), rewards (R), transition probabilities (P), discount factor (γ), and initial state (S_0) [21].

The robot utilizes a learning based model called GST + HH Attn [13], which employs an Attention mechanism [45] for navigation based on the past and current positions of humans to predict future positions.

In the GST + HH Attn model, the robot begins at S_0 and receives as state information: the robot’s current position (p_x, p_y) , velocity (v_x, v_y) , destination (g_x, g_y) , maximum velocity v_{max} , angle θ , and robot radius ρ , along with the set of i -th person’s current position information (p_x^i, p_y^i) at time t , denoted as u_i^t . i can vary from 0

to a maximum number of people, n_{max} . However, due to limitations in LiDAR range, the total number of people n in the received state by the robot might differ from n_{max} and can vary at each time t . In addition, the robot remembers the past positions of detected people up to a constant M steps, using the trajectory prediction algorithm (GST) to nonlinearly predict $\hat{u}_i^{t+1:t+K}$, the predicted positions of individuals from time $t+1$ to $t+K$.

Therefore, the GST + HH Attn model leverages the set of predicted positions $\hat{U}_i^{t+1:t+K} = [\hat{u}_0^{t+1:t+K}, \hat{u}_1^{t+1:t+K}, \dots, \hat{u}_n^{t+1:t+K}]$ up to constant K steps and the set of current positions $U^t = [u_0^t, u_1^t, u_2^t, \dots, u_n^t]$ of people to predict the overall dynamics of people through an Attention mechanism. It employs a type of recurrent neural network (RNN) called GRU to detect and process longterm dependencies, enabling a broader field of view [46]. The model focuses on nearby individuals while selecting actions. Furthermore, it receives feedback and updates its state for the next step based on the chosen actions. Besides, the study employs five learning based methods using the same model:

- DS-RNN: A model utilizing an RNN. It does not predict trajectories.
- No pred + HH Attn: Attention based model, excluding trajectory prediction ($r_{pred} = 0$).
- Const vel + HH Attn: An experimental case assumes that the trajectory prediction algorithm predicts trajectories to move at a constant velocity.
- Truth + HH Attn: An experiment assuming that the robot predicts the actual human trajectory.
- GST + HH Attn: Scenarios in which the robot predicts the human trajectory nonlinearly using the GST.

For a detailed model explanation, please refer to [13, 17].

Each human was randomly generated with a starting location and destination. Humans exchange their location information $U^t = [u_0^t, u_1^t, u_2^t, \dots, u_n^t]$ with each another and calculate velocities based on the positions, engaging in collision avoidance by altering their speed and direction using reactive based methods such as ORCA and SF [9-11].

Similar to robots, humans were designated destinations, and they aim to reach or modify them with a predetermined probability. Humans also possess attributes such as a size, speed, and maximum speed.

However, humans were assumed to disregard a robot’s location for two primary reasons. First, in crowded environments, human reactions to robots lead to subtle movements resulting in negligible positional changes. Even, rapid shifts are infeasible in densely populated settings. Second, encapsulating human dynamics within a mathematical model is challenging and can impede the learning process of robots. The diversity of the manners in which humans react to robots, along with associated uncertainties, makes modeling impractical. Furthermore, even if such modeling were feasible, it would interfere with the robot’s learning. As a result, humans do not perceive the robot’s location and ignore it.

Therefore, humans make their next actions based on their own characteristics, and information about the current positions and velocities of others.

3.2 Transformable Gaussian Reward Function (TGRF)

3.2.1 Formula and number of hyperparameters

TGRF leverages the characteristics of the normal distribution [47]. The normal distribution offers the advantage of being able to transform into various shapes with only two hyperparameters. This flexibility enhances the model’s adaptability, allowing adjustments to fit diverse prior knowledge and apply them to reward functions. Furthermore, it alleviates the burden on researchers in tuning hyperparameters, aiding in the swift identification of appropriate hyperparameters within a short time frame.

The formula for the normal distribution (N) is as follows:

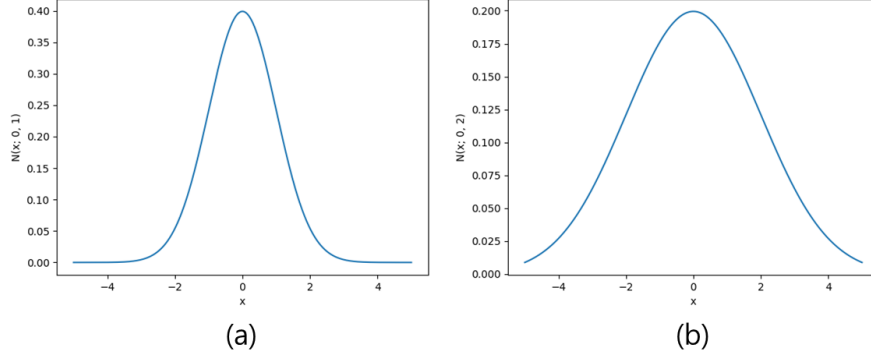


Fig. 3 Normal distribution. The X-axis denotes the X-value, and Y-axis represents the $N(x; \mu, \sigma)$. In (a), $\mu = 0, \sigma = 1$. In (b), $\mu = 0, \sigma = 2$.

$$N(x; \mu, \sigma) = \frac{1}{\sqrt{2\pi}\sigma} \cdot \exp\left(-\frac{(x - \mu)^2}{2\sigma^2}\right). \quad (1)$$

The normal distribution involves variables x , mean μ , and variance ρ . In Fig.3, the normal distribution represents the shape in which the values of a random variable are distributed, exhibiting symmetry around μ . It peaks at $x = \mu$ and decreases as x moves away from μ . ρ determines the width of the normal distribution, with the length of the width proportional to ρ . Therefore, the normal distribution has the advantage of being highly versatile in assuming various shapes with just two parameters, μ and ρ .

$$TGRF(w_{TGRF}, \mu_{TGRF}, \sigma_{TGRF}; x_{TGRF}) = \frac{w_{TGRF} \cdot N(x_{TGRF}; \mu_{TGRF}, \sigma_{TGRF})}{C_{\text{norm}}} \quad (2)$$

$$C_{\text{norm}} = \max_{x_{\text{norm}}} N(x_{\text{norm}}; \mu_{TGRF}, \sigma_{TGRF})$$

TGRF leverages characteristics of a normal distribution. In Equation (2), TGRF involves three hyperparameters: w_{TGRF} , representing the weight of TGRF; μ_{TGRF} , denoting the mean; and ρ_{TGRF} , indicating the variance.

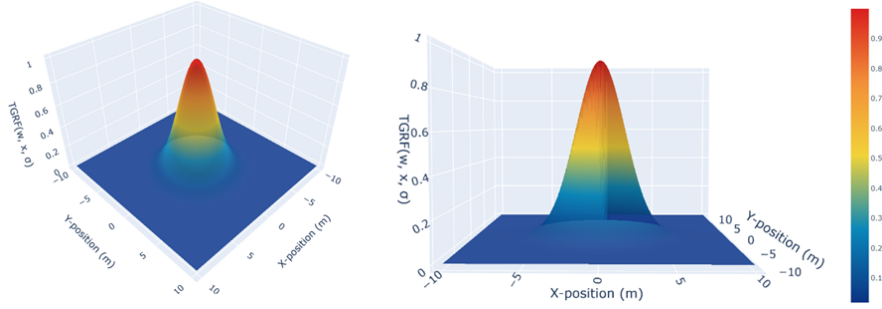


Fig. 4 TGRF. The X-axis denotes the X-position in meters, the Y-axis represents the Y-position in meters, and the Z-axis indicates TGRF value when $w_{TGRF} = 1, x_{TGRF} = dist(X, Y), \mu_{TGRF} = 0, \sigma_{TGRF} = 2$.

It incorporates a single variable x_{TGRF} . C_{norm} ensures that TGRF attains a maximum value of 1 irrespective of ρ_{TGRF} . This allows the scaling of TGRF solely by w_{TGRF} , enabling researchers to intuitively control its maximum value, preventing the freezing robot problem [43], and balancing it with other reward values to attain the desired algorithmic performance ultimately.

ρ_{TGRF} determines the transformability of TGRF. As $\lim_{\sigma_{TGRF} \rightarrow \infty} \mathcal{N}(x_{TGRF}; \mu_{TGRF}, \sigma_{TGRF})$, it takes on a constant form insensitive to changes in x_{TGRF} , while as $\lim_{\sigma_{TGRF} \rightarrow 0} \mathcal{N}(x_{TGRF}; \mu_{TGRF}, \sigma_{TGRF})$, it resembles an impulse function. This versatility enables the creation of diverse forms such as constant, linear, non-linear, Gaussian, etc., adaptable to specific objectives.

μ_{TGRF} determines the position of TGRF's maximum value. Thus, it allows adjustments of the maximum value position according to the objectives requiring specific values to be reached. The variable x_{TGRF} signifies the variable in $\mathcal{N}(x_{TGRF}; \mu_{TGRF}, \rho_{TGRF})$. As a result, it ultimately represents a shape similar to Fig. 4.

3.2.2 Transformability

The reward functions in Section II-B had different formulas and limited flexibility. These constraints lead to complexity in the reward functions and difficulty in determining the optimal performance. Therefore, researchers must redesign and tune them to achieve better performances. However, the TGRF offers versatility in generating various shapes.

Fig. 5 illustrates the creation of different shapes using the same TGRF by simply adjusting ρ_{TGRF} . Fig. 5a results in a TGRF that generates a continuous Gaussian distribution, making it suitable for moving objects or humans by applying varying penalties. Moreover, Fig. 5b forms a discrete column like shape. This configuration is suitable for stationary reward functions or objects. This approach allows various shapes via adjusting only a hyperparameter (ρ_{TGRF}) without requiring an additional function. This significantly reduces the researchers' time and effort while enabling finetuning to match the specific characteristics of objects.

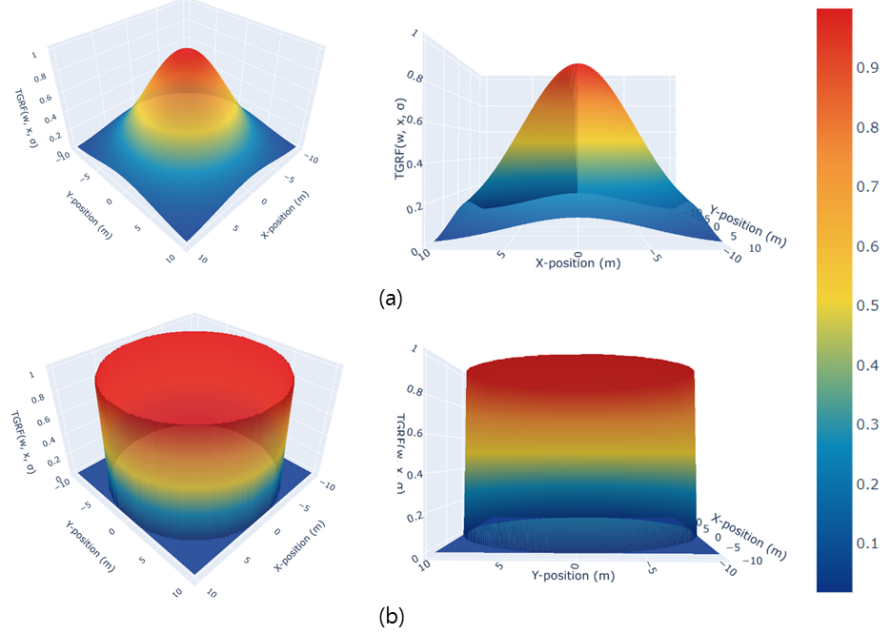


Fig. 5 Transformability of TGRF. The X-axis denotes the X-position in meters, the Y-axis represents the Y-position in meters, and the Z-axis indicates TGRF value. In (a), $w_{TGRF} = 1, x_{TGRF} = dist(X, Y), \mu_{TGRF} = 0, \sigma_{TGRF} = 5$. In (b), $w_{TGRF} = 1, x_{TGRF} = dist(X, Y), \mu_{TGRF} = 0, \sigma_{TGRF} = 5000$.

3.2.3 Reward function

Reward $r(s_t, a_t)$ is categorized into five types. First, $r_{goal}(s_t) = +10$ represents the reward when the robot successfully reaches its destination. Second, $r_{col}(s_t) = -10$ serves as a penalty incurred upon colliding with another individual. Third, $r_{disc}(s_t)$ represents a penalty for entering a danger zone. Fourth, $r_{pot}(s_t)$ corresponds to the reward/penalty contingent on the change in distance to destination S_{goal} . Finally, $r_{pred}(s_t)$ denotes the penalty invoked when entering a prediction.

Penalty $r_{disc}(s_t)$ is imposed when the robot enters the danger zone (d_{min} is within d_{disc}) determined by the nearest human distance, denoted as d_{min} . The formula is as follows:

$$r_{disc}(s_t) = TGRF(w_{disc}, 0, \sigma_{disc}; d_{min}) \quad (3)$$

In (3) and Fig. 6a, $r_{disc}(s_t)$ is designed to prevent collisions with humans, following a gaussian distribution with $\mu_{disc}=0$, whereby smaller values of d_{min} (closer proximity to humans) result in a higher penalty. This design aligns with prior knowledge and exhibiting a more plausible and realistic shape.

$r_{disc}(s_t)$ can be adjusted using only two hyperparameters. By tuning ρ_{disc} , researchers can regulate the breadth of the gaussian penalty concerning the distance between humans and the robot. This enables the robot to react more sensitively or less sensitively to the distance from humans. w_{disc} directly scales the reward function,

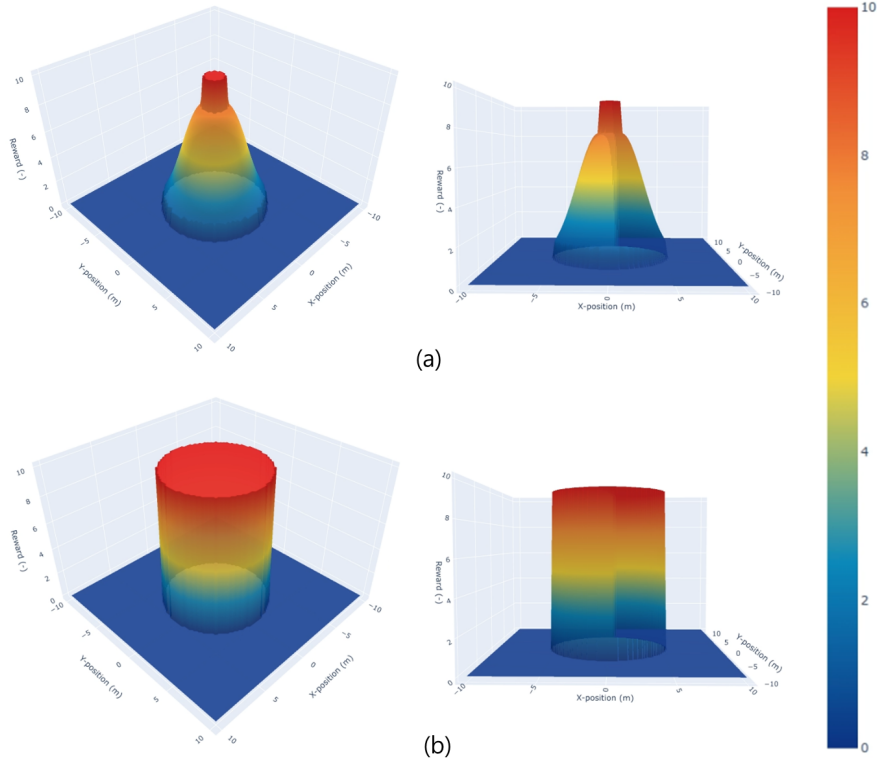


Fig. 6 TGRF applied to reward functions. The X-axis denotes the X-position in meters, the Y-axis represents the Y-position in meters, and the Z-axis indicates negative reward value. The central cylinder represents r_{col} , and the surrounding distribution represents $r_{disc}(s_t)$. Beyond d_{disc} , $r_{disc}(s_t)$ becomes 0 ($s_t \notin S_{danger}$ zone). In (a), $w_{TGRF} = 8, x_{TGRF} = dist(X, Y), \mu_{TGRF} = 0, \sigma_{TGRF} = 3$. In (b), $w_{TGRF} = 10, x_{TGRF} = dist(X, Y), \mu_{TGRF} = 0, \sigma_{TGRF} = 1000$.

establishing a linear correlation with $r_{disc}(s_t)$, thereby enabling the adjustment of the overall reward balance to prioritize driving tasks.

Potential reward $r_{pot}(s_t)$ represents the reward associated with the potential field, and is defined as follows:

$$r_{pot}(s_t) = \Delta d \cdot TGRF(1.5, \mu_{pot}, \sigma_{pot}; \mu_{pot}) \quad (4)$$

$$\Delta d = (-d_{goal}^t + d_{goal}^{t-1})$$

$r_{pot}(s_t)$ plays a crucial role in guiding a robot toward its destination and mitigating the freezing robot problem [21]. However, high values of $r_{pot}(s_t)$ can lead to increased collision rates with humans. Therefore, in equation (4), by setting $x_{pot} = \mu_{pot}$, we aimed to maintain a constant TGRF regardless of μ_{pot} and ρ_{pot} . In addition, by applying $w_{pot}=1.5$, we ensured equal weighting for all Δd , aiming for uniformity across them.

Penalty $r_{pred}(s_t)$ is the reward for the prediction and defined as follows:

$$\begin{aligned}
r_{\text{pred}}^i(s_t) &= \min_{k=1, \dots, K} \left(\mathbb{1}_i^{t+k} \frac{r_{\text{col}}}{2^k} \right) \\
r_{\text{pred}}(s_t) &= \min_{i=1, \dots, n} r_{\text{pred}}^i(s_t)
\end{aligned} \tag{5}$$

$r_{\text{pred}}(s_t)$ is used only in some models employing trajectory prediction. $r_{\text{pred}}(s_t)$ denotes the penalty value when the robot is positioned in the trajectory of the i -th person. $\mathbb{1}_i^{t+k}$ indicates whether the robot exists at the predicted position of the i -th person at time $t+k$ or not. Thus, $r_{\text{pred}}(s_t)$ takes the smallest penalty among all individuals' trajectory penalties that the robot takes. In our experiments, to demonstrate the performance enhancement even with different reward functions, we adopted $r_{\text{pred}}(s_t)$ used in the GST + HH Attn from [13]. The final definition of our reward function is as follows:

$$r(s_t, a_t) = \begin{cases} +10, & \text{if } s_t \in S_{\text{goal}} \\ -10, & \text{if } s_t \in S_{\text{collision}} \\ r_{\text{pred}}(s_t) + r_{\text{disc}}(s_t), & \text{if } s_t \in S_{\text{danger zone}} \\ r_{\text{pred}}(s_t) + r_{\text{pot}}(s_t), & \text{otherwise} \end{cases} \tag{6}$$

In summary, the TGRF offers the distinct advantage of intuitively and efficiently modifying the reward function with fewer hyperparameters. This enables the robot to make rational decisions and reduces the time consuming task of fine-tuning.

4 Simulation Experiments

This section describes the experimental setup, procedure, and outcomes.

4.1 Experimental environment

We employed a 2D environmental simulator used in previous studies [13]. This simulator features a 12×12 m space, with a 360° field of view and 5m sensor range for the light detection and ranging (LiDAR). We used a fixed number of humans (20) to represent a crowded setting.

$$\begin{aligned}
p_x[t+1] &= p_x[t] + v_x[t]\Delta t \\
p_y[t+1] &= p_y[t] + v_y[t]\Delta t
\end{aligned} \tag{7}$$

Both humans and robot operated using holonomic kinematics to determine their velocities ($a_t = [v_x, v_y]m/s$) along the x- and y-axes. Holonomic kinematics refers to a state where degrees of freedom can move independently without any constraints. This implies that robots and machines can move without any limitations on their position or orientation. As a result, the action space of a robot is continuous, allowing both robots and humans to immediately achieve their desired speed within a time frame of Δt , assuming they operate within the maximum speed limit. Therefore, the positions of the humans and robots were continuously updated according to (7).

The robot has attributions such as a size of $\rho = 0.3m$ and maximum speed of $v_{max} = 1.0m/s$. Humans also have characteristics such as a size ranging from 0.3 to 0.5m

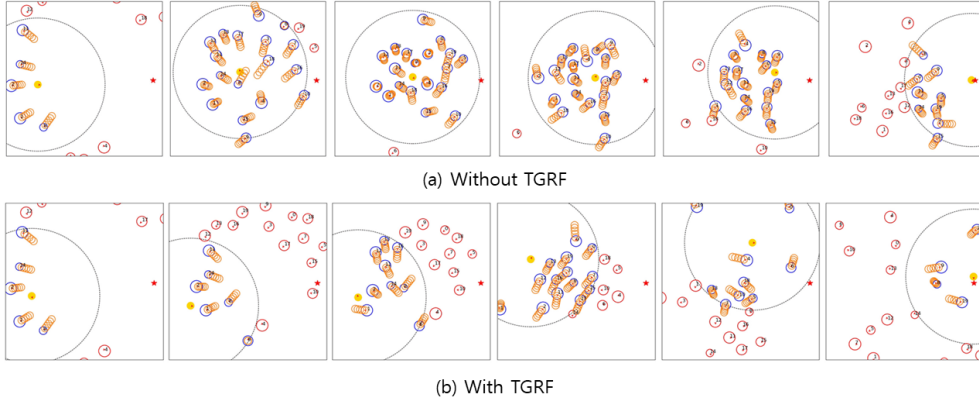


Fig. 7 Comparing a scenario with TGRF and a scenario without TGRF. Yellow circles represent robots, blue circles represent humans within the sensor range, red circles represent humans outside the sensor range, and orange circles in front of the blue circles indicate trajectories predicted by the GST.

and maximum speed varying between 0.5 and 1.5m/s. In addition, the locations and destinations of the robot were randomized, with the destinations not set excessively close. If the robot collides with an individual, reaches its destination, or exceeds the maximum time T , the episode is terminated, leading to the beginning of the subsequent episode.

Random seeding was applied during training, resulting in varying outcomes for each training episode. To handle the varying outcomes, multiple training runs were conducted with a total time step of 2×10^7 for the DS-RNN and 1×10^7 for the other algorithms. The learning rate was set to 4×10^{-5} for all policies. Subsequently, we acquired test data from 500 test episodes. The evaluation metrics applied to the test data included the success rate (SR), average navigation time (NT) in seconds, path length (PL) in meters for successful episodes, and intrusion time ratio (ITR).

4.2 Results

4.2.1 Results in different navigation methods and environment

We compared the performance of rewards (from section III-B-3) when the TGRF was applied to the performance without its application (reward function from [13]). The experiment involved the application of five different navigation methods for robots, as mentioned in Section III-A-1. Table I shows the performance when individuals adhere to ORCA, while Table II outlines the performance when adhering to SF. The hyperparameters are set to $w_{disc} = 0.25$, $x_{disc} = d_{min}$, $\mu_{disc} = 0$, $\rho_{disc} = 0.2$, $d_{disc} = 0.5$, $w_{pot} = 1.5$, $x_{pot} = \mu_{pot}$, $\mu_{pot} = 0$, $\rho_{pot} = 1000$. Through Table 1, 2, and Fig. 7, we were able to identify the three impacts of TGRF.

First, the TGRF results in a higher performance. As shown in Tables I and II, the TGRF outperformed significantly in terms of the SR. Notably, Table I shows that the

Table 1 Navigation results using the reward function from [13] and TGRF. Humans follow ORCA.

Reward	Navigation Method	Mean(sigma) of SR	SR(%)	NT(s)	PL(m)	ITR(%)
Without TGRF	DS-RNN	35.5 (7.697)	44.0	20.48	20.58	15.45
	No pred + HH Attn	59.636 (4.848)	67.0	17.49	20.30	17.22
	Const vel + HH Attn	65 (8.023)	81.0	17.34	21.95	6.15
	Truth + HH Attn	5.545 (1.616)	5.0	21.60	23.89	14.83
	GST + HH Attn	77.1 (5.718)	88.0	14.18	20.19	7.38
With TGRF (Ours)	DS-RNN	30.5 (4.843)	40.0	27.11	25.19	12.19
	No pred + HH Attn	59.364 (6.692)	72.0	18.17	21.92	14.16
	Const vel + HH Attn	87.909 (3.029)	92.0	16.38	22.33	5.08
	Truth + HH Attn	84.909 (4.776)	92.0	17.13	22.52	5.30
	GST + HH Attn	94.091 (2.843)	97.0	17.63	23.81	3.92

Table 2 Navigation results using the reward function from [13] and TGRF. Humans follow SF.

Reward	Navigation Method	Mean(sigma) of SR	SR(%)	NT(s)	PL(m)	ITR(%)
Without TGRF	DS-RNN	29.8 (5.231)	36.0	23.26	27.13	13.38
	No pred + HH Attn	12.091 (8.062)	28.0	26.52	34.98	12.78
	Const vel + HH Attn	92.182 (3.588)	96.0	14.74	21.49	5.24
	GST + HH Attn	91.636 (2.267)	95.0	13.74	20.47	5.37
With TGRF (Ours)	DS-RNN	48.6 (9.013)	62.0	22.48	25.26	10.14
	No pred + HH Attn	77.364 (6.079)	87.0	16.19	21.95	13.43
	Const vel + HH Attn	95.273 (1.911)	98.0	17.00	23.55	5.39
	GST + HH Attn	92.909 (3.579)	96.0	15.37	21.91	5.81

TGRF achieves an average SR of 94.091%, whereas the reward function without TGRF attains only 77.1% in the GST + HH Attn policy, marking a notable 17% increase.

Hence, models employing the TGRF generally exhibit equal or superior performances in terms of the SR and ITR. This implies that TGRF demonstrates relatively high performance across various models. This signifies that TGRF effectively incorporates prior knowledge based on the role of the reward function, indicating resilience in the freezing robot problem [43]. As a result, it is evident that the robot demonstrates high SR by taking appropriate actions according to the situation.

Second, even when combined with different reward functions without TGRF, TGRF exhibits high performance. In Tables I and II, for models utilizing trajectory prediction, $r_{pred}(s_t)$ employed the previous paper’s reward function without TGRF. Nonetheless, it showcased superior performance compared to [13], proving its adaptability to other reward functions.

Third, this leads to an enhanced recognition of human intent and collision avoidance. In Fig. 7a, the behavior of the robot when a reward function without TGRF was applied. The robot evidently struggles when confronted with a gathering crowd. Notably, in the test cases, the robot ventured into a crowd, resulting in unintended collisions with humans while attempting to navigate the crowd. Similar situations occurred in the other test cases. This means that the robot select aggressive or impolite

behaviors, such as sidestepping to avoid human and unintentional collisions, or making risky decisions to reach a destination faster, resulting in collisions. This behavior reflects a deficiency in understanding the broader intentions of humans and imbalance of the reward functions.

However, in Fig. 7b, the robot proactively positions itself behind the crowd before converging at a single point. This means that the values of $r_{pred}(s_t)$, $r_{pot}(s_t)$, and $r_{disc}(s_t)$ related to human interactions were well balanced, enabling the robot to navigate effectively without colliding with individuals.

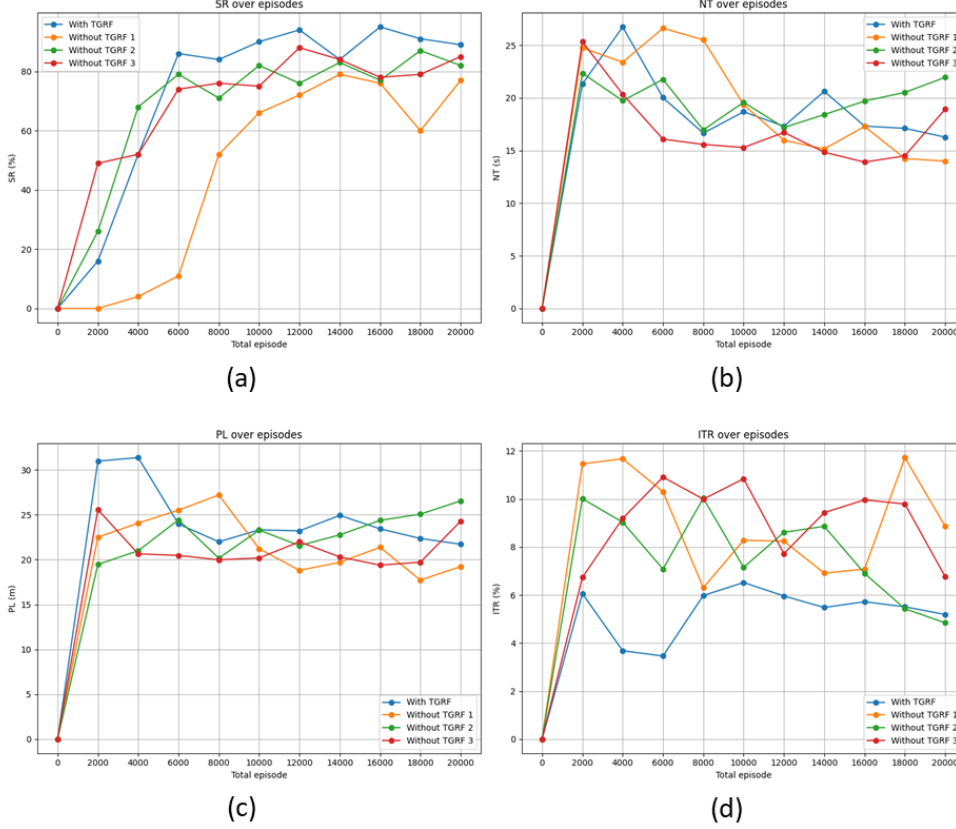


Fig. 8 Comparison of performance among four types of reward functions. The blue represents the reward function incorporating TGRF, while the orange corresponds to the reward function in [13], the green reflects [16], and the red signifies [31]. (a) denotes SR, (b) represents NT, (c) stands for PL, and (d) signifies ITR.

This signifies that TGRF effectively incorporates prior knowledge, and its priorities are well integrated into the policy. It suggests that the algorithm’s performance can be further enhanced when TGRF is applied. Further evidence of this enhancement is reflected in the results in Tables I and II, where the average SR and standard deviation

show similar or superior performances compared with previous iterations. In other test cases, we could observe that the robot selected a more secure and effective route than a faster and more dangerous route.

4.2.2 Performance comparison with other reward functions

In this experiment, we conducted trials applying the reward functions from studies [13, 16, 31] introduced in Section II-B, along with the reward function incorporating TGRF described in Section III-B-3. The navigation method employed GST + HH Attn models. Participants adhered to the ORCA approach, recording SR, NT, PL, ITR every 2000 episodes. The total episodes conducted were 20000 for GST + HH Attn.

First, it was observed that applying TGRF to the model led to an overall performance improvement compared to other models. In Fig. 8a, the reward function with TGRF was able to drive the algorithm’s performance up to a maximum of 95% over 16000 total episodes. Conversely, other reward functions achieved a maximum of 90% SR. This indicates that TGRF harmonizes appropriately with other reward functions, assuming a shape that aligns with the role of rewards, thereby eliciting the algorithm’s maximum performance.

In Fig. 8b, it was noticed that in the model applying TGRF, NT decreased with repeated learning, ultimately confirming the second lowest NT. Correspondingly, in Fig. 8c, the second lowest PL was also observed. This is associated with ITR, as lower NT and PL imply the robot tolerating penalties due to $r_{disc}(s_t)$ to reach the destination, resulting in higher ITR. For instance, looking at the orange graph, the highest ITR along with the lowest NT and PL can be observed. As a result, in Fig. 7a, this leads to choosing shorter and riskier paths, increasing the likelihood of not understanding human intentions and a higher possibility of collisions. However, in Fig. 8d, the model incorporating TGRF maintains the lowest ITR in most cases. This demonstrates that by applying TGRF, it selects the most efficient and safe paths compared to other models while maintaining the highest SR, reflecting the intentions of the algorithm, as shown in the results of Fig. 7b.

Second, Fig. 8 demonstrated the significant advantage of TGRF in terms of learning speed compared to the reward function without TGRF. In Fig. 8a, it was observed that three models reached saturation from a total of 6000 episodes. At this point, the model applying TGRF achieved the highest SR. This indicates the contribution of TGRF to faster learning speeds.

However, the TGRF has limitation in crowded environments. It does not inherently enhance the performance of core algorithms. For certain policies, comparable performances were achieved, as shown in Tables I and II. This suggests that the TGRF expedites the algorithm to achieve an optimal performance rather than inherently enhancing the algorithm itself.

5 Real-World Experiments

This study extends beyond simulations to real-world experiments. The model, trained using the unicycle approach, was applied to a physical robot in a real environment.

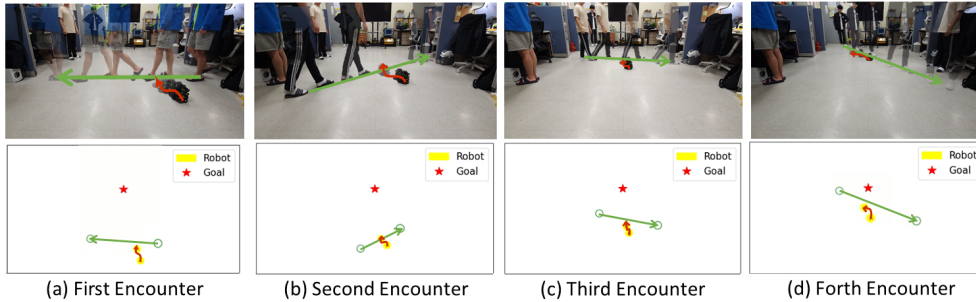


Fig. 9 Evasive actions performed by the robot in real-world scenarios and corresponding renderings with four humans (from left to right). The green arrows represent the movement path of the human, while the red arrows indicate the movement path of the robot. In addition, yellow circles indicate robots, green circles represent humans, and red stars indicate the destinations. These illustrations showcase the avoidance strategies employed by the robot as it encounters successive individuals: the (a) first, (b) second, (c) third, and (d) fourth human.

Unicycle kinematics present limitations in terms of direction and position control as compared to holonomic kinematics. Our experimental setup comprised a host computer equipped with an Intel i5-10600 processor @ 3.30 GHz and Nvidia RTX 3070 GPU; the robot utilized was a Turtlebot3. A LiDAR sensor, LDS-01, played a pivotal role in the human detection and robot position estimation. Robot positioning relied on SLAM localization, and human detection was accomplished using a 2D people detection algorithm based on 2D LiDAR data [35]. Detailed information can be accessed from <https://github.com/JinnnK/Tranformable-Gaussian-Reward-sim2real-with-Turtlebot3>.

Although our study assumed an absence of static obstacles other than humans, our real-world experiments were conducted in a confined space measuring approximately 3×5 m with static obstacles. These experiments involved scenarios in which the robot navigated between predefined start and destination points, encountering one to four pedestrians along its path. The maximum speed was approximately 0.6 m/s, and the investigation covered scenarios involving four moving individuals.

In Fig. 9a, the robot facing diagonally upward as the pedestrian moves from right to left. In this scenario, the robot rotates to the left, aligning with the pedestrian’s movement direction, instead of moving behind (to the right of) the human. This decision appears rational because both the destination and robot’s current orientation are oriented diagonally upward, making a leftward maneuver the most efficient choice when considering the human direction, speed, and destination. Notably, in another experiment involving three individuals, the robot was observed to halt temporarily instead of moving to the left.

In Fig. 9b, the robot encounters a pedestrian walking diagonally from left to right. In response, the robot navigates to the left to avoid obstructing the path of the pedestrian.

In Fig. 9c, the robot faces a human walking from left to right. Similarly, it predicts the human trajectory and executes a leftward turn to avoid a collision while approaching the destination.

In Fig. 9d, the robot encountered a human crossing diagonally from left to right near the destination. The robot smartly avoided the human by initially turning to the left, avoiding the pedestrian, and then turning to the right to reach the destination.

These actions underscore the robot’s ability to make real time decisions based on a dynamic environment, considering factors such as the human path, velocity, and proximity to the destination. The robot’s avoidance strategies prioritize efficiency while maintaining safety, and are influenced by various factors, including its current orientation and overall context of the situation. These real-world experiments testify the model’s adaptability in complex and dynamic environments, where human-robot interactions demand responsive and context aware behavior. The comprehensive renderings and additional experimental videos are available on <https://youtu.be/9x24k75Zj5k?si=OtczdVXPUnbGwpv->.

Two primary limitations were encountered during this experiment. (1) Computation load: the use of DNNs for action and trajectory predictions significantly increases computational demands. Considering the number of pedestrians considered, particularly for trajectory prediction, the time required for the next action was approximately 0.22 s. This resulted in seemingly irregular robot movements and delayed pedestrian responses. (2) Physical constraints: the accuracy of human detection and prediction is affected by sensor noise, limitations in the detection performance, and challenges in determining human angles. These factors lead to the occasional misidentification of obstacles as humans or limitations in the precision of human location information, thereby reducing the accuracy of the trajectory prediction. In addition, noise from the LiDAR sensor and location information errors caused by the robot’s movement accumulated over time, resulting in inaccuracies in location values as the experiment progressed.

6 Conclusion and Further Works

This study proposed the TGRF tailored for robots navigating crowded environments. This reward function has three advantages: a good performance with few hyperparameters, versatility for various objectives, and faster learning and stabilization. These statements were improved by the success rates and algorithm’s ability to discern human intentions compared with previous reward functions.

However, challenges emerged in both the simulations and real-world experiments. In the simulations, these challenges involved sensitivity to hyperparameters, algorithmic limitations, a trade-off correlation between the SR and NT, and absence of static obstacles. In real-world tests, challenges include the sensor noise, and physical constraints.

Hence, in future research, (1) we will apply TGRF in various environments and with different objects. In this study, we demonstrated its performance limited to rewards concerning humans. Therefore, we plan to conduct experiments by applying TGRF to diverse objects such as walls, obstacles, drones, and more. (2) we intend to

devise TGRF considering physical limitations. While TGRF performs exceptionally well in ideal conditions, its performance decreases in reality due to computational load and physical issues. Hence, we aim to implement a dynamically adaptive TGRF that adjusts based on the situation by incorporating knowledge regarding these physical limitations.

Funding

This research was partly supported by the MSIT(Ministry of Science and ICT), Korea, under the Convergence security core talent training business support program(IITP-2023-RS-2023-00266615) supervised by the IITP(Institute for Information & Communications Technology Planning & Evaluation), and the BK21 plus program "AgeTech-Service Convergence Major" through the National Research Foundation (NRF) funded by the Ministry of Education of Korea[5120200313836], and Institute of Information & communications Technology Planning & Evaluation (IITP) grant funded by the Korea government(MSIT) (No.RS-2022-00155911, Artificial Intelligence Convergence Innovation Human Resources Development (Kyung Hee University)), and the Ministry of Trade, Industry and Energy (MOTIE), South Korea, under Industrial Technology Innovation Program under Grant 20015440, 20025094

References

1. Nourbakhsh, I.R., et al., Mobile robot obstacle avoidance via depth from focus. *Robotics and Autonomous Systems*, 1997. 22(2): p. 151-158.
2. Ulrich, I. and J. Borenstein. VFH+: Reliable obstacle avoidance for fast mobile robots. in *Proceedings. 1998 IEEE international conference on robotics and automation (Cat. No. 98CH36146)*. 1998. IEEE.
3. Nalpantidis, L. and A. Gasteratos, Stereovision-based fuzzy obstacle avoidance method. *International Journal of Humanoid Robotics*, 2011. 8(01): p. 169-183.
4. Nalpantidis, L., G.C. Sirakoulis, and A. Gasteratos, Non-probabilistic cellular automata-enhanced stereo vision simultaneous localization and mapping. *Measurement Science and Technology*, 2011. 22(11): p. 114027.
5. Pritsker, A.A.B., *Introduction to Simulation and SLAM II*. 1984: Halsted Press.
6. Grisetti, G., et al., A tutorial on graph-based SLAM. *IEEE Intelligent Transportation Systems Magazine*, 2010. 2(4): p. 31-43.
7. Ai, Y., et al., DDL-SLAM: A robust RGB-D SLAM in dynamic environments combined with deep learning. *IEEE Access*, 2020. 8: p. 162335-162342.
8. Cui, L. and C. Ma, SDF-SLAM: Semantic depth filter SLAM for dynamic environments. *IEEE Access*, 2020. 8: p. 95301-95311.
9. Borenstein, J. and Y. Koren, Real-time obstacle avoidance for fast mobile robots. *IEEE Transactions on systems, Man, and Cybernetics*, 1989. 19(5): p. 1179-1187.
10. Van Den Berg, J., et al. Reciprocal n-body collision avoidance. in *Robotics Research: The 14th International Symposium ISRR*. 2011. Springer.
11. Helbing, D. and P. Molnar, Social force model for pedestrian dynamics. *Physical review E*, 1995. 51(5): p. 4282.

12. Patel, U., et al., DWA-RL: Dynamically Feasible Deep Reinforcement Learning Policy for Robot Navigation among Mobile Obstacles, in 2021 IEEE International Conference on Robotics and Automation (ICRA). 2021. p. 6057-6063.
13. Shuijing Liu, P.C., Zhe Huang, Neeloy Chakraborty, Kaiwen Hong, and D.L.M. Weihang Liang, Junyi Geng, and Katharine Driggs-Campbell. Intention Aware Robot Crowd Navigation with Attention-Based Interaction Graph. 2023.
14. Chen, C., et al. Crowd-robot interaction: Crowd-aware robot navigation with attention-based deep reinforcement learning, in 2019 international conference on robotics and automation (ICRA). 2019. IEEE.
15. Van den Berg, J., M. Lin, and D. Manocha. Reciprocal velocity obstacles for real-time multi-agent navigation. in 2008 IEEE international conference on robotics and automation. 2008. Ieee.
16. Oh, J., et al., SCAN: Socially-Aware Navigation Using Monte Carlo Tree Search. 2022.
17. Liu, S., et al. Decentralized structural-rnn for robot crowd navigation with deep reinforcement learning, in 2021 IEEE International Conference on Robotics and Automation (ICRA). 2021. IEEE.
18. Kretzschmar, H., G. Grisetti, and C. Stachniss, Lifelong map learning for graph-based slam in static environments. KI-Künstliche Intelligenz, 2010. 24: p. 199-206.
19. Brown, N., Edward T. Hall: Proxemic Theory, 1966. Center for Spatially Integrated Social Science. University of California, Santa Barbara. <http://www.csiss.org/classics/content/13> Read, 2001. 18: p. 2007.
20. Rios-Martinez, J., A. Spalanzani, and C. Laugier, From proxemics theory to socially-aware navigation: A survey. International Journal of Social Robotics, 2015. 7: p. 137-153.
21. Bellman, R., A Markovian decision process. Journal of mathematics and mechanics, 1957: p. 679-684.
22. Hastings, W.K., Monte Carlo sampling methods using Markov chains and their applications. 1970.
23. Mnih, V., et al., Playing atari with deep reinforcement learning. arXiv preprint arXiv:1312.5602, 2013.
24. Sutton, R.S., Learning to predict by the methods of temporal differences. Machine learning, 1988. 3: p. 9-44.
25. Jeong, H., et al., Deep Reinforcement Learning for Active Target Tracking, in 2021 IEEE International Conference on Robotics and Automation (ICRA). 2021. p. 1825-1831.
26. Gleave, A., et al., Quantifying differences in reward functions. arXiv preprint arXiv:2006.13900, 2020.
27. Mataric, M.J., Reward functions for accelerated learning, in Machine learning proceedings 1994. 1994, Elsevier. p. 181-189.
28. Laud, A.D., Theory and application of reward shaping in reinforcement learning. 2004: University of Illinois at Urbana-Champaign.
29. Montero, E.E., et al., Dynamic warning zone and a short-distance goal for autonomous robot navigation using deep reinforcement learning. Complex & Intelligent Systems, 2023: p. 1-18.

30. Samsani, S.S. and M.S. Muhammad, Socially compliant robot navigation in crowded environment by human behavior resemblance using deep reinforcement learning. *IEEE Robotics and Automation Letters*, 2021. 6(3): p. 5223-5230.
31. Samsani, S.S., H. Mutahira, and M.S. Muhammad, Memory-based crowd-aware robot navigation using deep reinforcement learning. *Complex & Intelligent Systems*, 2023. 9(2): p. 2147-2158.
32. Choi, J., G. Lee, and C. Lee, Reinforcement learning-based dynamic obstacle avoidance and integration of path planning. *Intelligent Service Robotics*, 2021. 14: p. 663-677.
33. Liu, S., et al., Socially aware robot crowd navigation with interaction graphs and human trajectory prediction. *arXiv preprint arXiv:2203.01821*, 2022.
34. Pérez-D'Arpino, C., et al. Robot navigation in constrained pedestrian environments using reinforcement learning. in *2021 IEEE International Conference on Robotics and Automation (ICRA)*. 2021. IEEE.
35. Scholz, J., et al. Navigation Among Movable Obstacles with learned dynamic constraints. in *2016 IEEE/RSJ International Conference on Intelligent Robots and Systems (IROS)*. 2016. IEEE.
36. Cassandra, A.R. A survey of POMDP applications. in *Working notes of AAAI 1998 fall symposium on planning with partially observable Markov decision processes*. 1998.
37. Hu, Y., et al., Learning to utilize shaping rewards: A new approach of reward shaping. *Advances in Neural Information Processing Systems*, 2020. 33: p. 15931-15941.
38. Icarte, R.T., et al., Reward machines: Exploiting reward function structure in reinforcement learning. *Journal of Artificial Intelligence Research*, 2022. 73: p. 173-208.
39. Yuan, M., et al., Automatic Intrinsic Reward Shaping for Exploration in Deep Reinforcement Learning. *arXiv preprint arXiv:2301.10886*, 2023.
40. Zhang, S., et al. Average-reward off-policy policy evaluation with function approximation. in *international conference on machine learning*. 2021. PMLR.
41. Rucker, M.A., et al., Reward Shaping for Human Learning via Inverse Reinforcement Learning. *arXiv preprint arXiv:2002.10904*, 2020.
42. Goyal, P., S. Niekum, and R.J. Mooney, Using natural language for reward shaping in reinforcement learning. *arXiv preprint arXiv:1903.02020*, 2019.
43. Trautman, P. and A. Krause. Unfreezing the robot: Navigation in dense, interacting crowds. in *2010 IEEE/RSJ International Conference on Intelligent Robots and Systems*. 2010. IEEE.
44. Huang, Z., et al., Learning sparse interaction graphs of partially detected pedestrians for trajectory prediction. *IEEE Robotics and Automation Letters*, 2021. 7(2): p. 1198-1205.
45. Niu, Z., G. Zhong, and H. Yu, A review on the attention mechanism of deep learning. *Neurocomputing*, 2021. 452: p. 48-62.
46. Fu, R., Z. Zhang, and L. Li. Using LSTM and GRU neural network methods for traffic flow prediction. in *2016 31st Youth academic annual conference of Chinese association of automation (YAC)*. 2016. IEEE.

47. Goodman, N.R., Statistical analysis based on a certain multivariate complex Gaussian distribution (an introduction). *The Annals of mathematical statistics*, 1963. 34(1): p. 152-177.